+ MODEL
ARTICLE IN PRESS
+ MODEL

Available online at www.sciencedirect.com

ScienceDirect

Advances in Climate Change Research xxx (xxxx) xxx

www.keaipublishing.com/en/journals/accr/

Regional changes in extreme heat events in China under stabilized 1.5 °C and 2.0 °C global warming

ZHANG Gu-Wei [a], ZENG Gang [a,*], Vedaste IYAKAREMYE [a], YOU Qing-Long [b]

[a] Key Laboratory of Meteorological Disaster of Ministry of Education (KLME), Collaborative Innovation Center on Forecast and Evaluation of Meteorological Disasters (CIC-FEMD), Nanjing University of Information Science and Technology, Nanjing, 210044, China

[b] Department of Atmospheric and Oceanic Sciences, Institute of Atmospheric Sciences, Fudan University, Shanghai, 200433, China

Received 1 March 2020; revised 29 May 2020; accepted 31 August 2020

Abstract

Extreme heat events (EHEs) have a significant impact on the social economy and human health. China is a country with a large population and diverse terrain, and it is necessary to project future extreme heat changes in the sub-regions. This study used a specially designed dataset, the Community Earth System Model (CESM) simulations, namely CESM low-warming, to investigate the EHEs in China under 1.5 °C and 2.0 °C global warming. The results indicate that the regional mean warming over China will exceed the global average, about 1.63 °C and 2.24 °C in 1.5 °C and 2.0 °C warmer futures. Compared to the present-day (1976−2005), the frequency and duration of the EHEs in South China are projected to increase the most among the sub-regions. For example, the frequency of EHEs in South China at 1.5 °C and 2.0 °C warming will exceed 3 and 3.5 times the present-day level. However, when global warming rises from 1.5 °C to 2.0 °C, the increased impacts relative to the 1.5 °C warming level will be the lowest in South China (less than 40%), and the highest increased impacts are projected to appear in Northeast China (53%−84%) and Northwest China (53%−107%). The main reason for this situation is that compared with the 1.5 °C scenario, the upper zonal westerly in northern China weakens and the continental high pressure enhances under the 2.0 °C scenario. Therefore, limiting global warming at 1.5 °C instead of 2.0 °C is beneficial for eliminating extreme heat events, especially for Northeast China and Northwest China.

Keywords: China; Regional changes; Extreme heat events; 1.5 °C and 2.0 °C global warming; CESM low-warming

1. Introduction

The Intergovernmental Panel on Climate Change (IPCC, 2013) reported that the global mean temperature (GMT) had risen about 0.85 °C (0.65−1.06 °C) from 1880 to 2012. Seven years later in 2020, the World Meteorological Organization (WMO) declared that global warming had reached 1.1 °C in 2019 and 2010−2019 was the hottest decade on record (WMO, 2020). Rapid global warming will likely have huge negative impacts on the social economy and human health (Robine et al., 2008; Seneviratne et al., 2016; Zhang et al., 2020). To reduce these adverse impacts, in December 2015, the United Nations Framework Convention on Climate Change (UNFCCC) adopted the Paris Agreement, which provides a framework for global action to address climate change. At this meeting, the Paris Agreement set a target to keep global warming below 2.0 °C and to persist with efforts to hold the warming under 1.5 °C above preindustrial days (UNFCCC, 2015). Furthermore, the Special Report on Global Warming of 1.5 °C released in 2018 also claimed that limiting global warming to 1.5 °C instead of 2 °C, could “reduce the number of people both exposed to climate-related risks and susceptible to poverty by up to several hundred million by 2050” (IPCC, 2018). Consequently, the 1.5 °C and 2 °C issues have become major research (Schleussner et al., 2016; Sanderson et al., 2017; Shi et al., 2018; Fu et al., 2018; Hu et al., 2019).

* Corresponding author.
E-mail address: zenggang@nuist.edu.cn (ZENG G.).

Peer review under responsibility of National Climate Center (China Meteorological Administration).

https://doi.org/10.1016/j.accre.2020.08.003

The extreme heat events (EHEs) have significantly increased with global warming over the past decades (Smith et al., 2013; Yu et al., 2017; Zhang et al., 2020). Long-term EHEs will destroy infrastructure and overburdened electricity and water facilities, which will have a major impact on the social economy (Wilbanks et al., 2012). In developing countries, when global warming rises by 2 °C, elevated heat stress will cause work productivity loss by one month per year (Yu et al., 2019). While most importantly, exposure to extreme heat increases morbidity and mortality (Robine et al., 2008; Grumm, 2011; Fischer and Knutti, 2015). The 2003 heatwave broke the record for the hottest summer in Europe and killed more than 4000 people (Barriopedro et al., 2011). In 2010, about 55,000 people in Russia died as a result of the heatwave (Hoag, 2014).

China is a huge energy consumer and the most populous country in the world and its surface air temperature (SAT) has increased by 0.9−1.5 °C since 1909, which is higher than the global average (CTNARCC, 2015). Due to an aging population, high density and high mobility, and weak infrastructure for disaster prevention and mitigation, China is vulnerable to extreme climate events (Ding et al., 2010; Qin, 2015). Since this century, China has experienced several EHEs. In the summer of 2013, East China experienced the hottest August, and Shanghai broke the high-temperature record, which caused dozens of deaths (Sun, 2014). Ye et al. (2014) showed that EHEs in China have generally increased significantly, and the areas affected by severe events had expanded significantly since the 1990s. Due to the EHEs, the labor force during the summer's peak period could be reduced by more than 60% in China (Wang and Zhang, 2019). Thus, to formulate policies and adapt to climate change, it is necessary to quantify the potential impact of 1.5 °C and 2 °C warming on China.

Previous studies have extracted the output simulations from the Coupled Model Intercomparison Program Phase 5 (CMIP5) and selected the periods when global warming reached 1.5 °C and 2 °C under the specific Representative Concentration Pathway scenarios (Wang et al., 2017; Xu et al., 2017). For instance, the future changes in surface temperature in many areas in China will exceed the 1.5 °C and 2.0 °C thresholds earlier than the global warming (Chen et al., 2013; Fu et al., 2018; Shi et al., 2018). Huang et al. (2017) investigated the impacts of 1.5 °C and 2 °C warming on global drylands by using CMIP5 results and pointed out that the rising rate of surface temperature increases with the decrease in vegetation coverage. However, there are some drawbacks in using CMIP5 model outputs (James et al., 2017; Lin et al., 2018). In the CMIP5 simulation, global warming will only briefly reach 1.5 °C and 2 °C, and then continue to rise, which cause the impacts between the short-term and stable warming periods quite different, especially for regional investigations (James et al., 2017). The National Center for Atmospheric Research (NCAR) has released a set of climate simulations focused on the 1.5 °C and 2.0 °C issues, named Community Earth System Model (CESM) low-warming, which is based on a fully coupled model with equilibrium climates in 1.5 °C and 2.0 °C world. Unlike the warming periods derived from CMIP5 were increasing, the CESM low-warming simulations were designed particularly for 1.5 °C and 2.0 °C issues, which contain a 30-year period (2071−2100) that the global warming stabled at the specific thresholds. Based on the CESM low-warming datasets, some researchers have provided the future projections in EHEs over China (Li et al., 2018; Yang et al., 2018; Lin et al., 2018; Chen and Sun, 2019), and they found that the increased temperature in 1.5 °C and 2.0 °C periods over China were projected to be about 10% higher than the global average, and the EHEs would increase significantly with stronger impacts under 2.0 °C warming. However, a major problem is that they mostly consider China as a whole region and rarely discuss the projections in sub-regions in China. Since ecological environments and economies in different regions could respond differently to global warming, it is necessary to investigate the future changes in EHEs over sub-regions in China.

This study mainly focuses on the regional future projections in the EHEs in China under 1.5 °C and 2.0 °C global warming and tends to address the following questions: 1) How will the EHEs change in different sub-regions in China? 2) Comparing 2.0 °C with 1.5 °C warming scenario, in which sub-region the EHEs will increase the most and how will the associated key atmospheric circulations change?

2. Data and methods

2.1. Observed data

China's daily observed SAT data (CN05, Wu and Gao, 2013) from 1961 to 2014, with 0.5° horizontal resolution, is used to correct the bias of simulated EHEs (Xu et al., 2009).

2.2. Model data

The NCAR CESM large-ensemble (CESM-LE) simulations are used to represent the historical data in 1850−2005 (Kay et al., 2015). All the simulations are conducted using the Community Atmosphere Model version 5 in CESM 1 (CESM1-CAM5) (Hurrell et al., 2013). The CESM1-CAM5 consists of coupled land, atmosphere, sea ice, and ocean component models (Lawrence et al., 2012; Moore et al., 2013; Kay et al., 2015). CESM-LE simulations include forty-two ensemble members, one of which is from 1850 to 2005, and the other 41 members are from 1920 to 2005. Details on CESM-LE can be found in Kay et al. (2015).

The NCAR CESM low-warming projections are used to analyze changes in 1.5 °C and 2.0 °C warmer futures. The Minimal Complexity Earth Simulator model (MiCES, 2016) is used to simulate the pathways of greenhouse gas to obtain a period of stable 1.5 °C and 2 °C above the preindustrial level (1850−1919). From 2006 to 2100, the emission pathways derived from MiCES are used in the 11 members of the future projections. All the forcings, such as ozone and aerosol emissions, follow the representative concentration pathway 8.5. The projections show a long period (2071−2100) of the global mean temperature stabilized at 1.5 °C and 2.0 °C above the preindustrial level. Details of the simulations can be found in Sanderson et al. (2017).

2.3. Period of preindustrial, present-day, 1.5 °C, and 2 °C

The years 1976–2005 represent present-day, and the preindustrial period is 1850–1919. The years 2071–2100 are referred to as the stable period for 1.5 °C and 2.0 °C global warming (Sanderson et al., 2017).

2.4. Extreme heat indices

Six extreme heat indices (Meehl and Tebaldi, 2004; Smith et al., 2013; Li et al., 2018) of 1976–2100 simulations are calculated (Table 1).

2.5. Bias-correction

The method described in Jung (2005) is adopted to correct bias in EHEs indices relative to CN05 data.

$$R_{\mathrm{BC}} = R_{\mathrm{Model}} - \Delta R \tag{1}$$

$$\Delta R = R'_{\mathrm{Model}} - R'_{\mathrm{Obs}} \tag{2}$$

Here, R_{Model} and R_{BC} are the projected and bias-corrected daily SAT, respectively; R'_{Obs} and R'_{Model} represent the average value of observed and projected data in 1976–2005, respectively; and ΔR represents the biases.

2.6. Probability ratio

The following formula is used to calculate the probability ratios (PR) (Yu et al., 2017; Li et al., 2018) of EHEs in different regions:

$$PR = P_1 / P_0 \tag{3}$$

Here, P_0 is the probability for the present-day (1976–2005), and P_1 is the probability for the future days (2071–2100).

2.7. Increased impacts

The increased impacts (IC) of EHEs caused by an additional 0.5 °C warming is investigated by using the following:

$$IC = [(C_{2.0} - C_{1.5}) / C_{1.5}] \times 100\% \tag{4}$$

where $C_{2.0}$ and $C_{1.5}$ represent the changes in 2.0 °C and 1.5 °C warming, respectively, relative to the present-day level.

2.8. Sub-regions

Owing to the diverse terrains of China, studying climate change extremes in the country is complicated. As in previous studies (Hu et al., 2019; Zhang et al., 2020; Zhao et al., 2020), we divide China into seven areas, Northwest China, Northeast China, Tibet, Southwest China, North China, Yangtze River Valley, and South China (Fig. 1). The extreme heat indices in each sub-region are calculated based on the model simulation data after bias-correction. Grids beyond the land of China are not considered.

3. Results

3.1. Evaluation of simulation results

The Taylor diagram (Taylor, 2001) is applied to evaluate the model performance against the results from the CN05 dataset. As shown in Fig. 2, the intensity indices (TXx and TNx) have a good performance in bias-corrected results, compared with the original simulation. Their standardized deviations and spatial correlations are close to 1. Furthermore, the climatological spatial distributions of bias-corrected results for TXx/TNx are also much more similar to the observations than the original simulations (Fig. A1). For example (Fig. A1), the original simulated TXx/TNx in eastern China and Tibet are lower than the observed, while the bias-corrected results are close to the observed. In some previous studies (Cannon et al., 2015; Ma et al., 2017; Li et al., 2018), the bias-correction method was found to have little effect on percentile-based indices, such as HW and WSDI. In our results (Fig. 2), the performances of the

Table 1
Definitions of extreme heat indices.

Acronym	Indicator	Definition	Unit
TXx	Warmest day	Maximum Tmax in a year	°C
TNx	Warmest night	Maximum Tmin in a year	°C
TX90p	Warm days	Annual number of days in which Tmax exceeds 90% of the present-day level	d
TN90p	Warm nights	Annual number of days in which Tmin exceeds 90% of the present-day level	d
WSDI	Warm spell duration indicator	Annual number of days with at least six consecutive days in which Tmax exceeds 90% percentile of the present-day level	d
HW	Heatwave	A heatwave is defined as a period in a year that satisfies all the following criteria: 1) at least three consecutive days with the Tmax exceeds 95% of the present-day level in summer (June–August); 2) the average Tmax of the entire period exceeds 95% percentile of the present-day level in summer; 3) Tmax for each day during the period exceeds 80% percentile of the present-day level in summer	d

Note: Tmax (Tmin) means daily maximum (minimum) SAT.

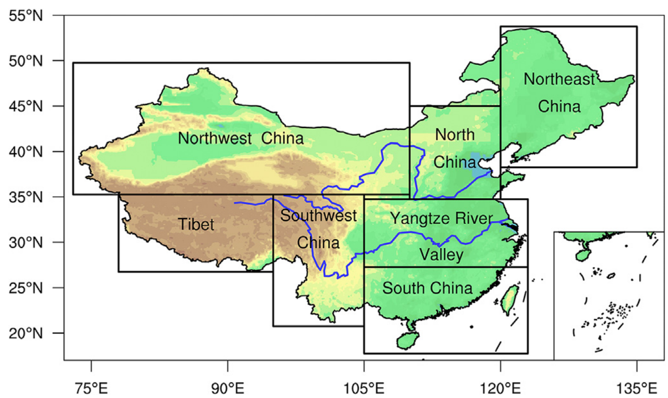

Fig. 1. Map showing the seven geographical divisions of China.

percentile-based indices (HW and WSDI) are not bad, although they are not much improved after bias-correction. Therefore, the bias-correction method can improve the performance of the EHE indices selected in this study.

3.2. Projected surface air temperature changes

Compared with the preindustrial level, the annual mean SATs over China under 1.5 °C and 2.0 °C warming are stabilized at about 1.63 °C and 2.24 °C from 2071 to 2100, respectively (Fig. 3a); these temperatures are approximately 10% higher than the global average (1.5 °C and 2.0 °C). The regional changes in mean SAT (Fig. 3b) show that the increases in most sub-regions will exceed the global average (except South China and Yangtze River Valley), and the maximum (minimum) value is projected to locate in Northeast China (South China), about 2.02 °C/2.74 °C (1.12 °C/1.50 °C) under 1.5 °C/2.0 °C warming. Fig. 3b also indicates that high-latitude and high-altitude areas of China, such as North China, Northeast China, Northwest China, and Tibet, project larger magnitudes of increase than other regions, which also supports the conclusion of Shi et al. (2018).

Fig. 4 shows the spatial patterns and regional average changes in the mean, maximum, and minimum SAT in the future. Relative to the present-day level, it is apparent that the maximum SAT is projected to rise more than the mean and minimum SAT. For example, under 2.0 °C warming, the maximum SAT (Fig. 4e) in most areas will increase at least 2.0 °C, while for the increases in mean and minimum SAT (Fig. 4b and h), only parts of western China will exceed 2.0 °C. In each sub-region (Fig. 4j and k), except Northwest China, the regional average increased amplitude in the maximum SAT is projected to be higher than the mean and minimum SAT. Comparing 2.0 °C warming with 1.5 °C warming, the over-0.5 °C warming pattern in maximum SAT (Fig. 4f) projects to locate in most areas of China, also larger than the results of the mean and minimum SAT (Fig. 4c and i). Thus, from present-day to 1.5 °C/2.0 °C global warming period, the maximum SAT will have more contribution to the warming than the mean and minimum SAT, which also means more high-temperature events will occur in the future.

Based on the percentile thresholds determined by the present-day (1976–2005) level, the regional mean probability ratios for the responses of daily maximum SAT to 1.5 °C and 2.0 °C global warming is given in Fig. 5. As displayed in Fig. 5, the extreme high-temperature probability ratio increases more than the moderately high-temperature probability ratio, and the values under 2.0 °C warming are higher than those under 1.5 °C warming. For China under 1.5 °C and 2.0 °C warming (Fig. 5a), the daily maximum SAT that higher than 95% of the present-day period is projected to be 3.6 and 4.4 times the present-day level, respectively. Among the seven

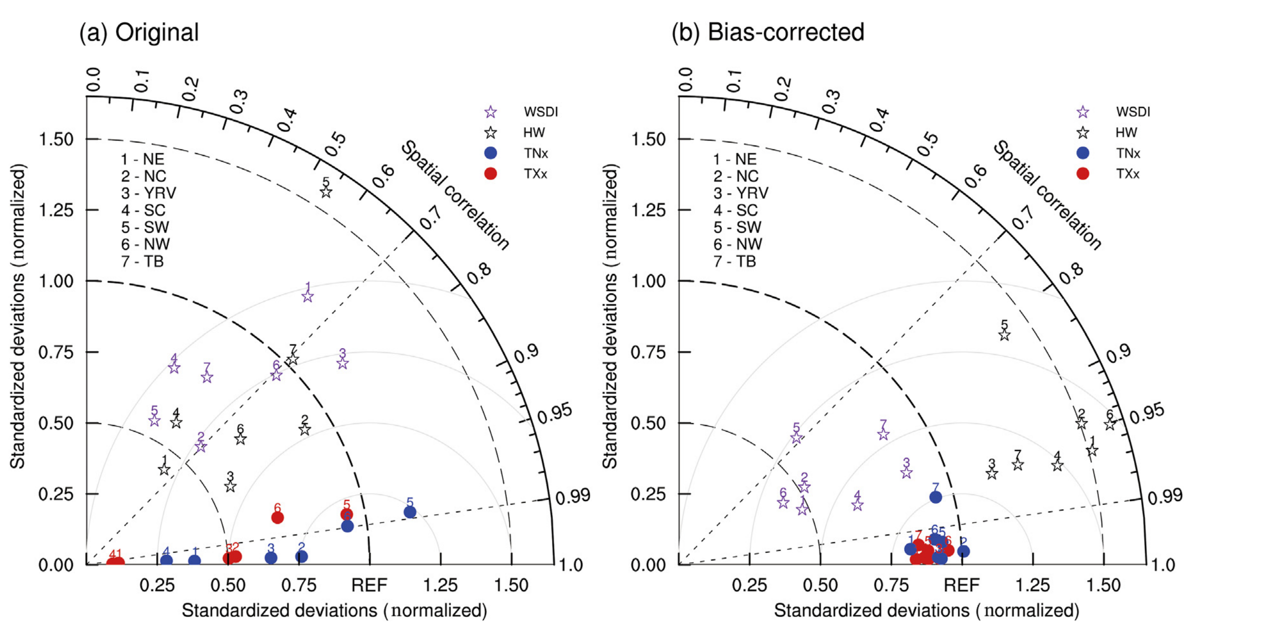

Fig. 2. The performances of (a) original simulated and (b) bias-corrected extreme heat events (EHEs) indices from the National Center for Atmospheric Research's Community Earth System Model (CESM large-ensemble) for TXx, TNx, HW, and WSDI as compared with CN05 data of 1976–2005.

Please cite this article as: ZHANG, G.-W., et al., Regional changes in extreme heat events in China under stabilized 1.5 °C and 2.0 °C global warming, Advances in Climate Change Research, https://doi.org/10.1016/j.accre.2020.08.003

+ MODEL

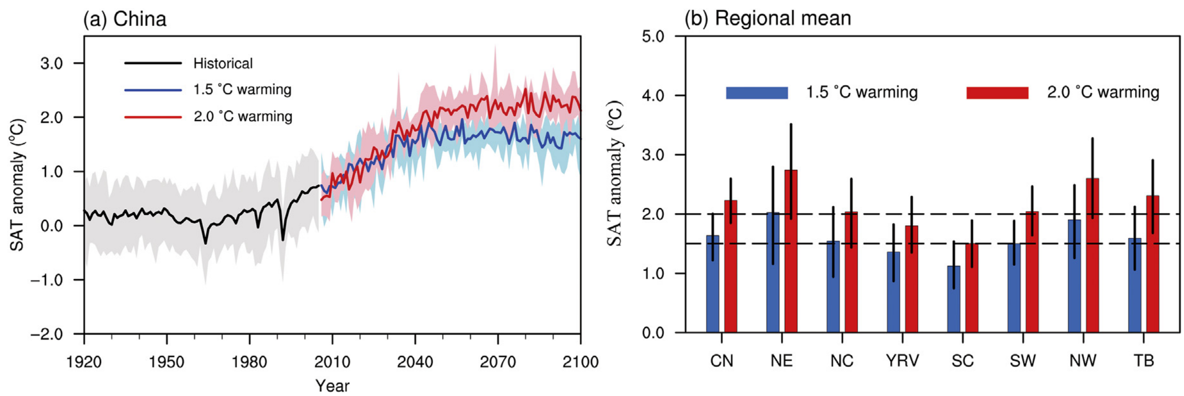

Fig. 3. (a) The annual mean SAT anomalies from 1920 to 2100 in China compared with the preindustrial (1850−1919) levels, and (b) regional mean changes in SAT under 1.5 °C and 2.0 °C warming (2071−2100) relative to the preindustrial period (The perpendicular black lines at the top of bars represent the variation between the minimum and maximum. CN, NE, NC, YRV, SC, SW, NW, and TB denote China, Northeast China, North China, Yangtze River Valley, South China, Southwest China, Northwest China, and Tibet, respectively).

sub-regions, the increases in probability ratios in South China, Southwest China, and Tibet are higher than in other sub-regions. The daily maximum SAT that higher than 95% of the present-day period in South China, Southwest China, and Tibet will exceed 5 and 6 times the present-day level at 1.5 °C and 2.0 °C warming.

3.3. Changes in extreme heat events

As shown in Fig. 6 and Fig. 7, the changes in the intensity (TXx and TNx) and frequency (TX90p and TN90) of EHEs relative to the present-day period indicate that the index calculated by the maximum SAT (TXx and TSX90p) will increase larger than the one calculated by the minimum SAT (TNx and TN90p). For example (Fig. 6 and Fig. A2), the TXx under 1.5 °C (2.0 °C) warming is projected to increase 0.7−1.7 °C (1.4−2.6 °C) relative to the present-day level, while the increase in TNx will be slightly lower, which is 0.7−1.4 °C (1.4−2.1 °C). Similarly, the increases in TN90p will be about 20% (relative to the present-day level) less than the increase in TX90p (Fig. 7 and Fig. A3).

Among the sub-regions, the changing magnitudes of the frequency and duration (HW and WSDI) show more significant regional differences than the results of intensity. Under 1.5 °C and 2.0 °C global warming, the TX90p (TN90p) across China will increase by 50%−230% (30%−230%) and 80%−270% (70%−250%). The regional mean changes (Fig. 7) and spatial results (Fig. A3) both indicate that the increased amplitudes of the high-temperature frequency in South China, Southwest China, and Tibet will exceed 100% and 150% of present-day level under 1.5 °C and 2.0 °C warming, higher than those in other sub-regions. Especially in South China (Fig. A3), the high-temperature frequency in 1.5 °C and 2.0 °C warmer future are projected to exceed 3 and 3.5 times the present-day level. For the duration extreme indices (Fig. 8), the HW (WSDI) under 1.5 °C and 2.0 °C warming across China are projected to increase 200%−700% (125%−600%) and 360%−900% (300%−700%) of the present-day level. The increases in HW (WSDI) for South China will also be the highest in 1.5 °C and 2.0 °C warmer futures, about 600%−700% (500%−600%) and 700%−900% (600%−700%) of the present-day level. The spatial results (Fig. A4) also show that the EHE duration days in almost the entire region of South China will increase by 40 and 60 in 1.5 °C and 2.0 °C scenarios.

When compared the 2.0 °C scenario with the 1.5 °C scenario, the increases in South China will not be the most. A further 0.5 °C warming from 1.5 °C to 2.0 °C will cause increases of 0.3−1.0 °C in TXx and 0.3−0.9 °C in TNx across China (Fig. 6c and f), and with the lowest growth rate in South China, about 0.3−0.6 °C. For the frequency (Fig. 7c and f) and duration (Fig. 8c and f) over seven sub-regions, the differences between 2.0 °C scenario and 1.5 °C scenario are projected to be about 12%−66% and 80%−330%, while the results for South China will be less than 50% and 150%.

We use the 1.5 °C warming as the reference to calculate the increased impacts in 2.0 °C warming, and the results are shown in Fig. 9. Relative to the 1.5 °C warming, the additional 0.5 °C warming will lead to a 35%−84% increase in the intensity of EHEs (TXx and TNx), 16%−66% increase in the frequency of EHEs (TX90p and TN90p), and 15%−107% in the duration of EHEs (HW and WSDI) across China. The lowest increased impacts are projected to locate in South China (less than 40%), and the largest increased impacts will occur in Northeast China (53%−84%) and Northwest China (53%−107%). The increased amplitude of intensity, frequency, and duration of EHEs over Northeast China and Northwest China under the 2.0 °C warming will be more than 70%, 50%, and 90% of those under 1.5 °C warming, respectively. Therefore, Northeast China and Northwest China are particularly sensitive to the additional 0.5 °C warming from 1.5 °C to 2.0 °C, and it is worthwhile for them to limit the global warming under 1.5 °C instead of 2.0 °C.

3.4. Differences of atmospheric circulations at additional 0.5 °C warming

Previous studies have pointed out that the upper zonal westerly and continental high pressure were closely related to changes in vertical movements and clouds; the changes can

Please cite this article as: ZHANG, G.-W., et al., Regional changes in extreme heat events in China under stabilized 1.5 °C and 2.0 °C global warming, Advances in Climate Change Research, https://doi.org/10.1016/j.accre.2020.08.003

+ MODEL

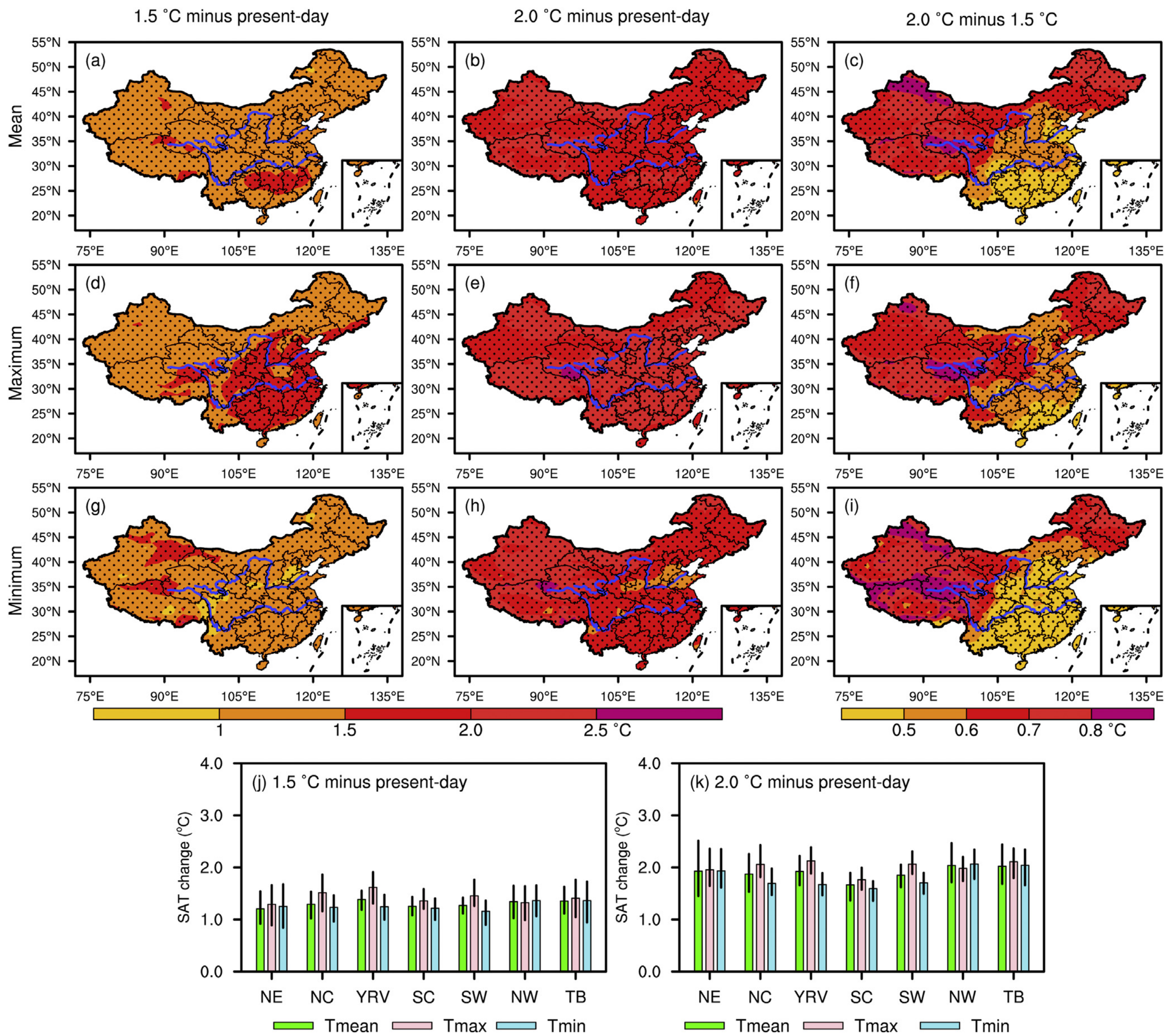

Fig. 4. Mean/maximum/minimum SAT changes (2071–2100) under 1.5 °C warming (a, d, g) and 2.0 °C warming (b, e, h) compared with the present-day (1976–2005) levels, and (c, f, i) the changes under 2.0 °C warming compared with those under 1.5 °C warming (Dotted areas are statistically significant at the 0.05 level). Regional mean changes under 1.5 °C warming (j) and 2.0 °C warming (k) compared with the present-day level (The perpendicular black lines at the top of bars represent the variation between the minimum and maximum. NE, NC, YRV, SC, SW, NW, and TB denote Northeast China, North China, Yangtze River Valley, South China, Southwest China, Northwest China, and Tibet, respectively).

affect radiation, precipitation, and other processes, which can eventually lead to summer high-temperature changes in northern China (Lu et al., 2001; Sun, 2014; Zhang et al., 2020). Compared to the 1.5 °C warming, the EHEs in Northwest China and Northeast China will increase the most among the sub-regions under 2.0 °C warming. This section aims to briefly describe the differences in atmospheric circulations in summer that contribute to this situation.

The correlation patterns of the EHEs indices in Northeast China and Northwest China with the summer zonal wind at 200 hPa (U200) and geopotential height at 500 hPa (Z500) under the two warming scenarios are similar (Fig. A5 and Fig. A6). The significant negative correlations are at about 40 °N in the results of U200, which is the location of the upper zonal westerly. Furthermore, the significant positive correlations are located over Northeast China and Northwest China in the results of Z500, which is the location of the continental high pressure. Thus, under 1.5 °C and 2.0 °C warming, the atmospheric circulation systems closely related to EHEs are still the upper zonal westerly and continental high pressure, which is consistent with the present-day period. The wind differences of U200 between the two warming scenarios (Fig. 10a) indicate the upper zonal westerly is weakened over Northeast China and Northwest China under 2.0 °C warming. The weakened summer upper zonal westerly will cause the temperature in Northwest China and Northeast China to rise (Lu et al., 2001; Zhang et al., 2020), which can be a reason that more EHEs under 2.0 °C warming. Furthermore, positive

Please cite this article as: ZHANG, G.-W., et al., Regional changes in extreme heat events in China under stabilized 1.5 °C and 2.0 °C global warming, Advances in Climate Change Research, https://doi.org/10.1016/j.accre.2020.08.003

+ MODEL

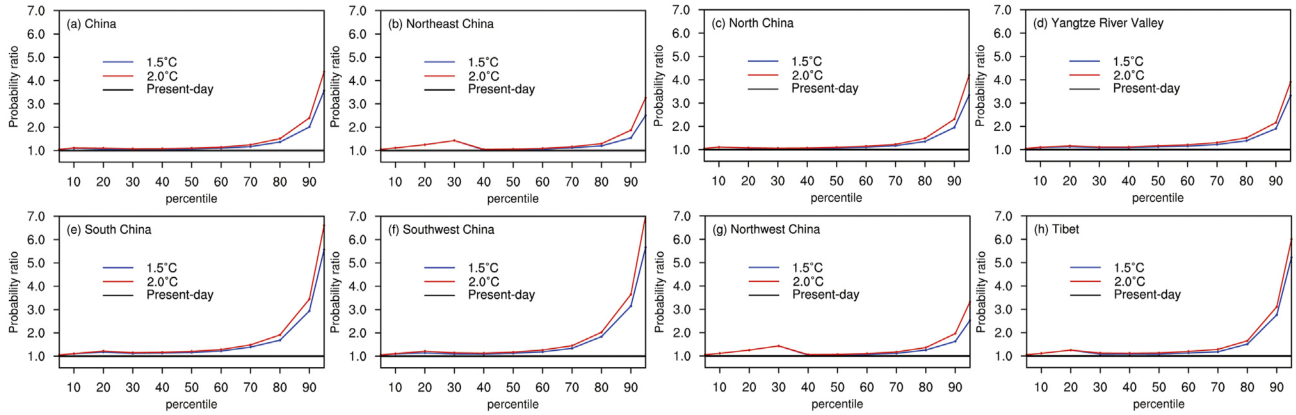

Fig. 5. Regional mean probability ratios (2071–2100) for the responses of daily maximum SAT to 1.5 °C and 2.0 °C global warming based on the percentile thresholds determined by the present-day (1976–2005) levels.

differences of summer Z500 are observed over Northeast China and Northwest China (Fig. 10b), indicating the continental high pressure is enhanced under 2.0 °C warming compared with that under 1.5 °C warming. The summer geopotential height in the high-latitude regions (e.g. Northeast China and Northwest China) will increase much higher than that in the low-latitude regions (e.g., South China). The enhanced geopotential height indicates more clear sky weather, which is conducive to temperature rise (Sun, 2014; Zhang et al., 2020). Thus, more increases in the geopotential height in the high-latitude areas can also be a reason for the large increases in the EHEs in Northeast China and Northwest China when the global warming rises from 1.5 °C to 2 °C.

4. Discussion

Some new insights can be drawn from our analysis, including under 1.5 °C and 2.0 °C warming, the highest increases in frequency and duration of EHEs relative to the present-day level will locate in South China, while Northeast China and Northwest China will be more sensitive to the additional warming of 0.5 °C (from 1.5 °C to 2.0 °C).

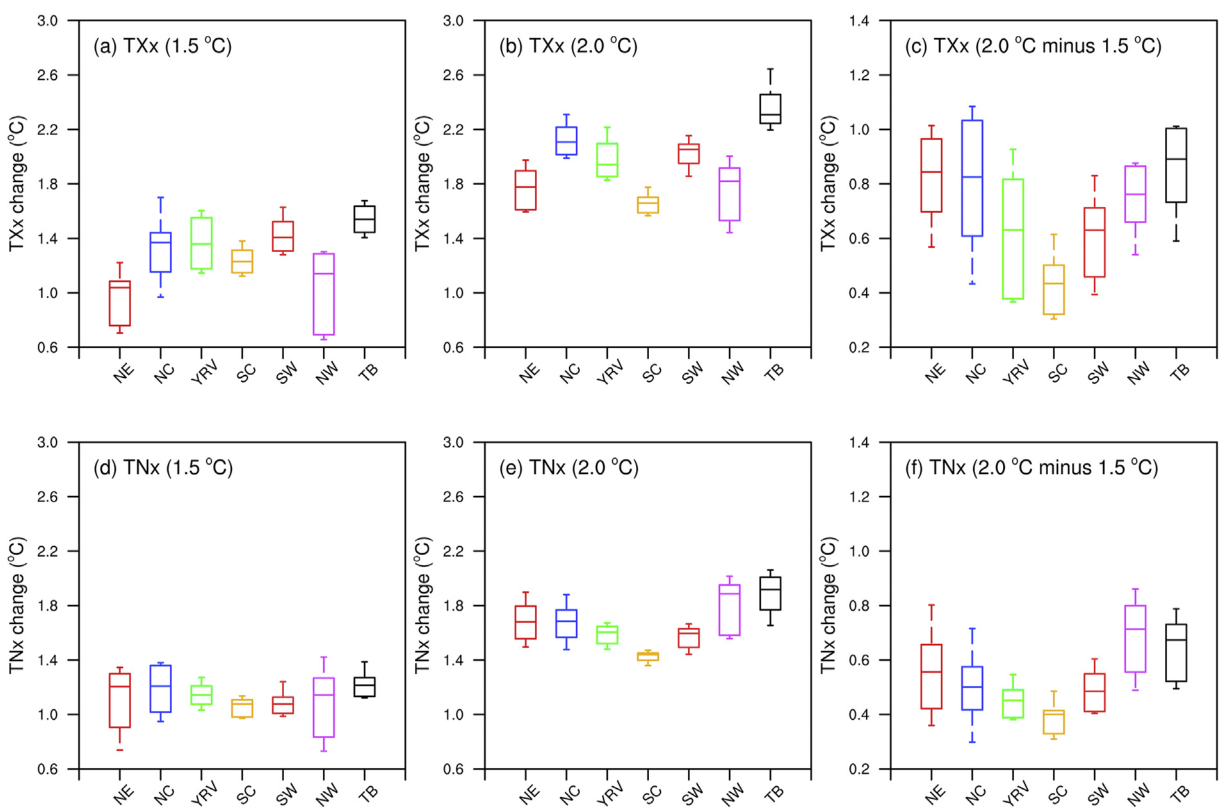

Fig. 6. Regional mean changes (2071–2100) in TXx/TNx under (a, d) 1.5 °C warming and (b, e) 2.0 °C warming relative to the present-day levels, and (c, f) 2.0 °C warming relative to 1.5 °C (The box whisker plots are the 25th, 33.3th, 50th, 66.7th, and 75th intervals. NE, NC, YRV, SC, SW, NW, and TB denote Northeast China, North China, Yangtze River Valley, South China, Southwest China, Northwest China, and Tibet, respectively).

Please cite this article as: ZHANG, G.-W., et al., Regional changes in extreme heat events in China under stabilized 1.5 °C and 2.0 °C global warming, Advances in Climate Change Research, https://doi.org/10.1016/j.accre.2020.08.003

+ MODEL

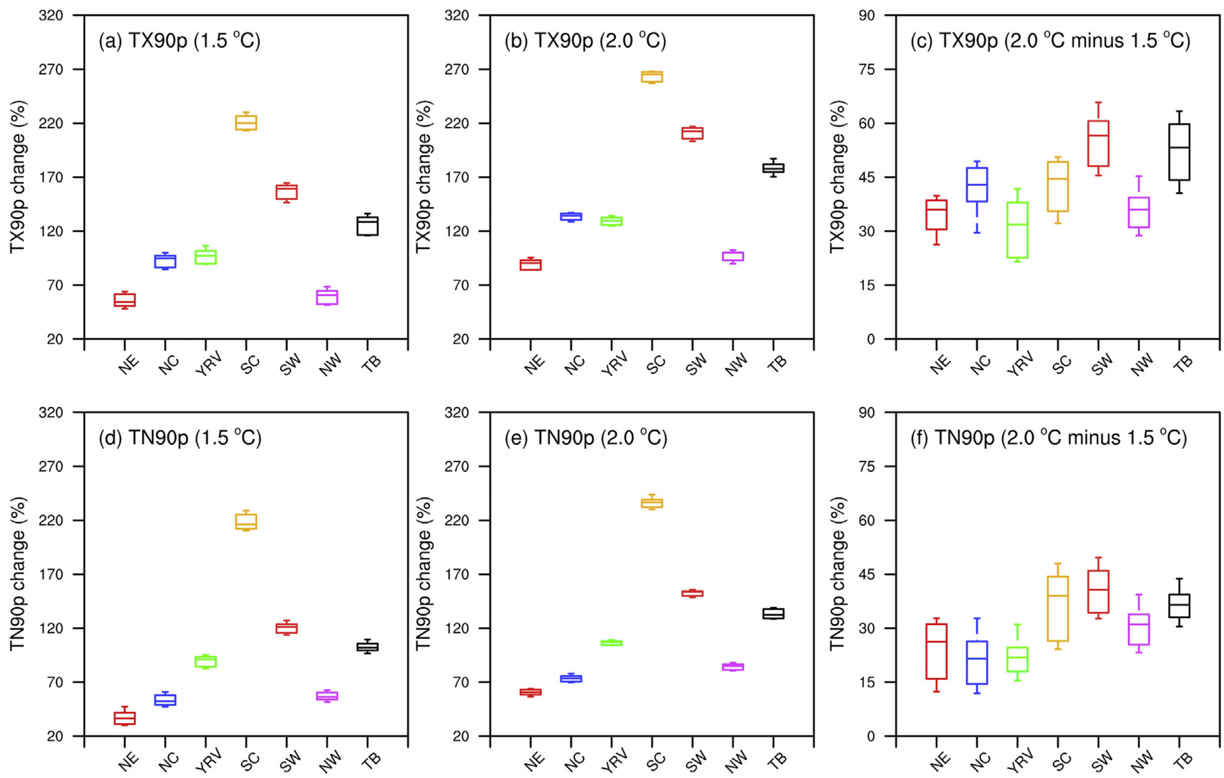

Fig. 7. Regional mean changes (2071−2100) in TX90p/TN90p under (a, d) 1.5 °C warming and (b, e) 2.0 °C warming relative to the present-day levels, and (c, f) 2.0 °C warming relative to 1.5 °C (The box whisker plots are the 25th, 33.3th, 50th, 66.7th, and 75th intervals. NE, NC, YRV, SC, SW, NW, and TB denote Northeast China, North China, Yangtze River Valley, South China, Southwest China, Northwest China, and Tibet, respectively).

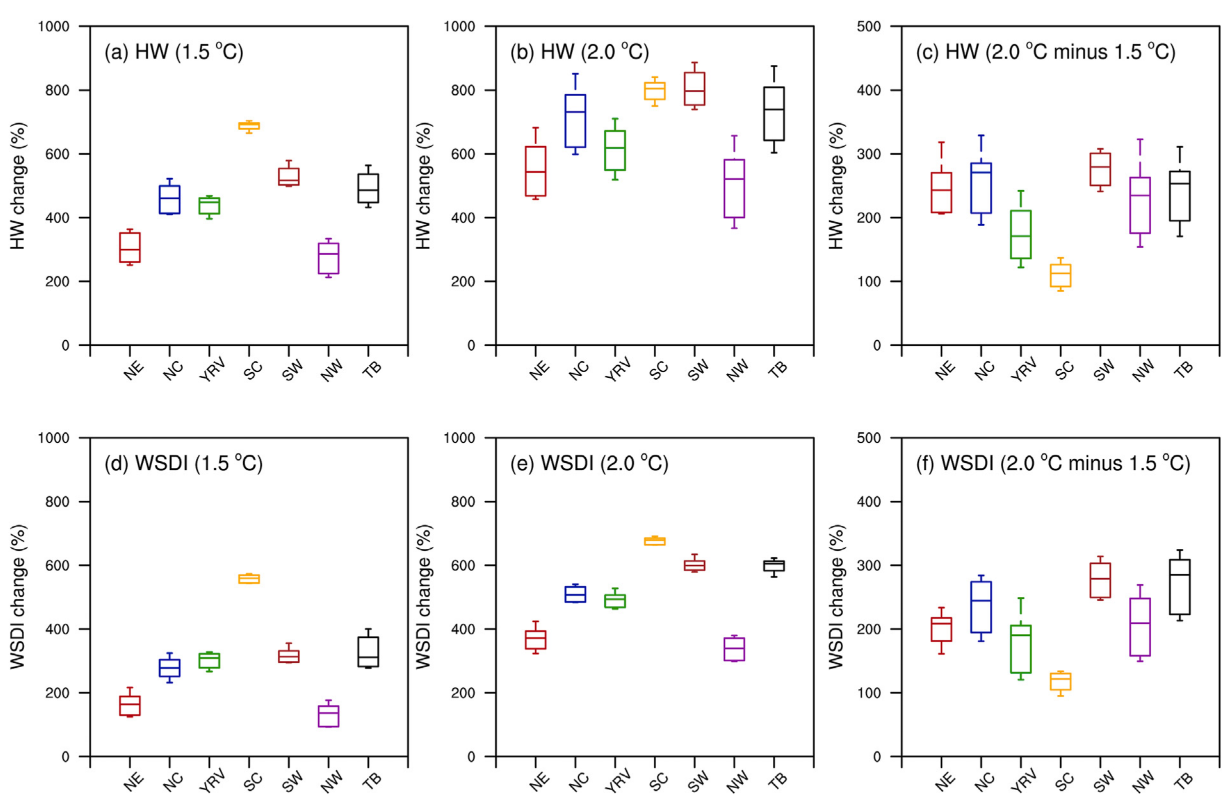

Fig. 8. Regional mean changes (2071−2100) in HW/WSDI under (a, d) 1.5 °C warming and (b, e) 2.0 °C warming relative to the present-day levels, and (c, f) 2.0 °C warming relative to 1.5 °C (The box whisker plots are the 25th, 33.3th, 50th, 66.7th, and 75th intervals. NE, NC, YRV, SC, SW, NW, and TB denote Northeast China, North China, Yangtze River Valley, South China, Southwest China, Northwest China, and Tibet, respectively).

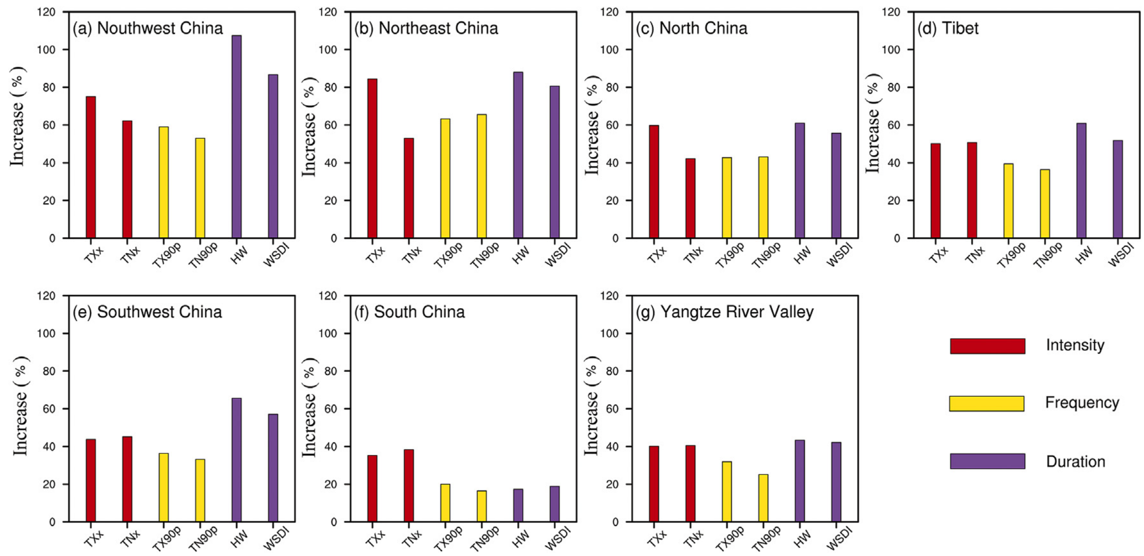

Fig. 9. The increased impacts of EHEs in sub-regions at 2.0 °C compared with those at 1.5 °C warming.

However, there are still some limitations. For instance, the bias-correction method used in this study has not improved much performance on the duration extreme indices (WSDI and HW), and this is also in line with Li et al. (2018). To obtain more reliable results in future projection, it is important to reduce the bias of the model. Thus, various bias-correction methods (e.g., machine learning; Grover et al., 2019) and dynamic downscaling method (e.g., CWRF; Liang et al., 2019) should be used to further study. Additionally, the warming over China under 1.5 °C and 2.0 °C this scenario in our study are 1.63 °C and 2.24 °C, relatively lower than those studies using CMIP5 outputs (1.7−2.0 °C and 2.4−2.7 °C, Fu et al., 2018). It's probably caused by different model designs. As concluded in Lin et al. (2018), the CESM low-warming simulations were more in line with the scenario set by the Paris Agreement. However, only one fully coupled climate model (CESM) simulation is not enough. More climate models are needed to perform stable warming projections, and the multi-model results will be more convincing. Furthermore, it is worth studying the impacts of extreme high temperatures on humans, nature, and social economy (Fischer et al., 2012; Lee and Min, 2018; He et al., 2017). We have found that South China would face the frequency of EHEs exceeding 600%/700% of the present-day level under 1.5 °C/2.0 °C warming. As a densely populated and economically developed area (Jiang et al., 2017, 2018; Zhu et al., 2020), it is necessary to investigate the impacts on the population and the economy caused by high temperatures in South China. Meanwhile, for Northeast China and Northwest China, as the largest forestry area and the arid areas in China (Tao et al., 2013; Huang et al., 2017), the EHEs under 2.0 °C warming will be hugely different with those under 1.5 °C warming. Continuous exposure to high temperatures may increase the frequency and intensity of forest fires, and the likelihood of tree deaths caused by droughts and high temperatures worldwide may increase (Allen et al., 2004). Moreover, warming will also boost evaporation, which dries out the soil and exacerbates drought (Chai et al., 2018; Miralles et al., 2018). Increasing drought will affect agricultural products in Northwest China, such as wheat and cotton (Wang et al., 2008). Thus, quantifying the future risks caused by high temperatures in Northeast China and Northwest China, such as forest fires (Li et al., 2019) and drought (Huang et al., 2017), are also worthwhile.

In summary, this study projected future EHE changes in China's sub-regions under 1.5 °C and 2.0 °C warming, which can provide the basis for an in-depth regional study.

5. Conclusions

For climate change adaption and international climate negotiations, it is essential to understand how the regional climate responds to the 1.5 °C and 2.0 °C global warming. Here, we used the CESM low-warming simulations to project future changes in extreme heat events (EHEs) over China's sub-regions. The conclusions are summarized as follows:

(1) Under 1.5 °C and 2.0 °C warming scenarios, our results show that warming over China (1.63 °C and 2.24 °C) will exceed the global average, especially in Northeast China (2.02 °C and 2.74 °C). The simulations also project that the extreme temperature indices calculated by maximum temperature (e.g. TXx and TX90p) will increase more than those calculated by minimum temperature (e.g. TNx and TN90p).
(2) Compared to the present-day period (1976−2005), the EHEs across China will increase about 0.7−1.7 °C (1.4−2.6 °C) in intensity, 30%−230% (70%−270%) in frequency, and 125%−700% (360%−900%) in duration under 1.5 °C (2.0 °C) global warming. Besides, the increased magnitudes of the frequency and duration in South China will be the largest. The high-temperature frequency in South China is projected to exceed 3 and

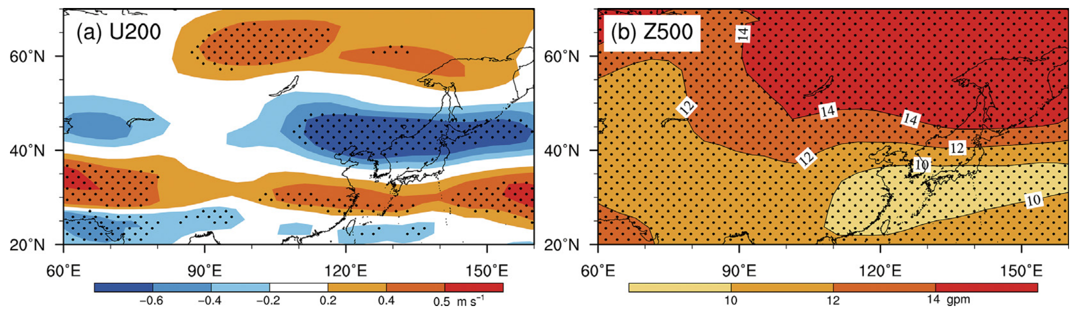

Fig. 10. Climatological differences of 200 hPa zonal wind (a) and (b) geopotential height at 500 hPa in summer from 2071 to 2100 between the 2 °C and 1.5 °C scenarios (Dotted areas are statistically significant at the 0.05 level).

3.5 times the present-day level at 1.5 °C and 2.0 °C warmer future, and the duration of EHEs, such as heatwave, will extend more than 600%−700% and 700%−900% of the present-day level.

(3) Compared 2.0 °C global warming with 1.5 °C global warming, an additional 0.5 °C warming will lead the intensity, frequency, and duration of EHEs increase by 35%−84%, 16%−66%, and 15%−107% across China, respectively. The lowest increased impacts are projected to occur in South China (less than 40%), and the highest increased impacts will be in Northeast China (53%−84%) and Northwest China (53%−107%). Under 2.0 °C warming, the increases in intensity, frequency, and duration of EHEs over Northeast China and Northwest China will be 1.5−2 times the 1.5 °C warming level. The reason for this can be the weakening of the zonal westerly and the enhanced continental high pressure over northern China in the 2.0 °C warming, compared to the 1.5 °C warming. Therefore, it is beneficial for China, especially for Northwest China and Northeast China, to limit global warming under 1.5 °C instead of 2.0 °C.

Declaration of Competing Interest

The authors declare no conflict of interest.

Acknowledgments

This research is supported by the National Key Research and Development Program of China (2017YFA0603804), the National Natural Science Foundation of China (41430528 and 41831174).

Appendix A. Supplementary data

Supplementary data to this article can be found online at https://doi.org/10.1016/j.accre.2020.08.003.

References

Allen, M., Booth, B., Frame, D., et al., 2004. Observational constraints on future climate: distinguishing robust from model-dependent statements of uncertainty in climate forecasting, vol. 11. IPCC Risk and Uncertainty Workshop, Maynooth, Ireland.

Barriopedro, D., Fischer, E.M., Luterbacher, J., et al., 2011. The hot summer of 2010: redrawing the temperature record map of Europe. Science 332 (6026), 220−224. https://doi.org/10.1126/science.1201224.

Cannon, A.J., Sobie, S.R., Murdock, T.Q., 2015. Bias correction of GCM precipitation by quantile mapping: how well do methods preserve changes in quantiles and extremes? J. Clim. 28 (17), 6938−6959. https://doi.org/10.1175/jcli-d-14-00754.1.

Chai, R., Sun, S., Chen, H., et al., 2018. Changes in reference evapotranspiration over China during 1960-2012: attributions and relationships with atmospheric circulation. Hydrol. Process. 32 (19), 3032−3048. https://doi.org/10.1002/hyp.13252.

Chen, H., Sun, J., 2019. Increased population exposure to extreme droughts in China due to 0.5°C of additional warming. Environ. Res. Lett. 14, 064011 https://doi.org/10.1088/1748-9326/ab072e.

Chen, H., Sun, J., Chen, X., 2013. Projection and uncertainty analysis of global precipitation-related extremes using CMIP5 models. Int. J. Climatol. 34 (8), 2730−2748. https://doi.org/10.1002/joc.3871.

CTNARCC (Committee for China's Third National Assessment Report on Climate Change), 2015. The Third National Assessment Report on Climate Change. Science Press, Beijing (in Chinese).

Ding, T., Qian, W., Yan, Z., 2010. Changes in hot days and heat waves in China during 1961-2007. Int. J. Climatol. 30 (10), 1452−1462. https://doi.org/10.1002/joc.1989.

Fischer, E.M., Oleson, K.W., Lawrence, D.M., 2012. Contrasting urban and rural heat stress responses to climate change. Geophys. Res. Lett. 39 (3), L03705. https://doi.org/10.1029/2011gl050576.

Fischer, E.M., Knutti, R., 2015. Anthropogenic contribution to global occurrence of heavy-precipitation and high-temperature extremes. Nat. Clim. Change 5 (6), 560−564. https://doi.org/10.1038/nclimate2617.

Fu, Y., Lu, R., Guo, D., 2018. Changes in surface air temperature over China under the 1.5 and 2.0 °C global warming targets. Adv. Clim. Change Res. 9 (2), 112−119. https://doi.org/10.1016/j.accre.2017.12.001.

Grover, A., Song, J., Kapoor, A., et al., 2019. Bias correction of learned generative models using likelihood-free importance weighting. Adv. Neural Inf. Process. Syst. 11058−11070.

Grumm, R.H., 2011. The central European and Russian heat event of July−August 2010. Bull. Am. Meteorol. Soc. 92 (10), 1285−1296. https://doi.org/10.1175/2011BAMS3174.1.

He, L., Cleverly, J., Wang, B., et al., 2017. Multi-model ensemble projections of future extreme heat stress on rice across southern China. Theor. Appl. Climatol. 133 (3−4), 1107−1118. https://doi.org/10.1007/s00704-017-2240-4.

Hoag, H., 2014. Russian summer tops 'universal' heatwave index. Nature 16 (4). https://www.nature.com/news/russian-summer-tops-universal-heatwave-index-1.16250.

Hu, W., Zhang, G., Zeng, G., et al., 2019. Changes in extreme low temperature events over northern China under 1.5°C and 2.0°C warmer future scenarios. Atmosphere 10 (1), 1. https://doi.org/10.3390/atmos10010001.

Huang, J., Yu, H., Dai, A., et al., 2017. Drylands face potential threat under 2 °C global warming target. Nat. Clim. Change 7 (6), 417−422. https://doi.org/10.1038/nclimate3275.

Hurrell, J.W., Holland, M.M., Gent, P.R., et al., 2013. The community earth system model: a framework for collaborative research. Bull. Am. Meteorol. Soc. 94, 1339−1360. https://doi.org/10.1175/bams-d-12-00121.1.

IPCC, 2013. Climate Change 2013: The Physical Sciences Basis. Contribution of Working Group I to the Fifth Assessment Report of the Intergovernmental Panel on Climate Change. Cambridge University Press, Cambridge and New York.

IPCC, 2018. Warming of 1.5°C. http://www.ipcc.ch/Sr15.

James, R., Washington, R., Schleussner, C.F., et al., 2017. Characterizing half-a-degree difference: a review of methods for identifying regional climate responses to global warming targets. Climatic Change 8 (2), e457. https://doi.org/10.1002/wcc.457.

Jiang, T., Zhao, J., Jing, C., et al., 2017. National and provincial population projected to 2100 under the shared socioeconomic pathways in China. Clim. Change. Res. 13 (2), 128−137 (in Chinese).

Jiang, T., Zhao, J., Cao, G.L., et al., 2018. Projection of national and provincial economy under the shared socioeconomic pathways in China. Clim. Change. Res. 14 (1), 50−58 (in Chinese).

Jung, T., 2005. Systematic errors of the atmospheric circulation in the ECMWF forecasting system. Q. J. R. Meteorol. Soc. 131 (607), 1045−1073. https://doi.org/10.1256/qj.04.93.

Kay, J.E., Deser, C., Phillips, A., et al., 2015. The community earth system model (CESM) large ensemble project: a community resource for studying climate change in the presence of internal climate variability. Bull. Am. Meteorol. Soc. 96 (8), 1333−1349. https://doi.org/10.1175/bams-d-13-00255.1.

Lawrence, P.J., Feddema, J.J., Bonan, G.B., et al., 2012. Simulating the biogeochemical and bio geophysical impacts of transient land cover change and wood harvest in the Community Climate System Model (CCSM4) from 1850 to 2100. J. Clim. 25 (9), 3071−3095. https://doi.org/10.1175/JCLI-D-11-00256.1.

Lee, S.M., Min, S.K., 2018. Heat stress changes over East Asia under 1.5 and 2.0 C global warming targets. J. Clim. 31 (7), 2819−2831. https://doi.org/10.1175/JCLI-D-17-0449.s1.

Li, D., Zhou, T., Zou, L., et al., 2018. Extreme high-temperature events over East Asia in 1.5°C and 2°C warmer futures: analysis of NCAR CESM low-warming experiments. Geophys. Res. Lett. 45, 1541−1550. https://doi.org/10.1002/2017gl076753.

Li, X., Jin, H., He, R., et al., 2019. Effects of forest fires on the permafrost environment in the northern Da Xing'anling (Hinggan) Mountains, Northeast China. Permafr. Periglac. Process. 30 (3), 163−177. https://doi.org/10.1002/ppp.2001.

Liang, X.Z., Sun, C., Zheng, X., et al., 2019. CWRF performance at downscaling China climate characteristics. Clim. Dynam. 52 (3−4), 2159−2184. https://doi.org/10.1007/s00382-018-4257-5.

Lin, L., Wang, Z., Xu, Y., et al., 2018. Additional intensification of seasonal heat and flooding extreme over China in a 2°C warmer world compared to 1.5°C. Earth's Future 6 (7), 968−978. https://doi.org/10.1029/2018ef000862.

Lu, R., Oh, J.H., Kim, B.J., et al., 2001. Associations with the interannual variations of onset and withdrawal of the Changma. Adv. Atmos. Sci. 18 (6), 1066−1080. https://doi.org/10.1007/s00376-001-0023-3.

Ma, S., Zhou, T., Angélil, et al., 2017. Increased chances of drought in southeastern periphery of the Tibetan Plateau induced by anthropogenic warming. J. Clim. 30 (16), 6543−6560. https://doi.org/10.1175/jcli-d-16-0636.1.

Meehl, G.A., Tebaldi, C., 2004. More intense, more frequent, and longer lasting heat waves in the 21st century. Science 305 (5686), 994−997. https://doi.org/10.1126/science.1098704.

MiCES (Minimal Complexity Earth Simulator), 2016. GitHub repository. https://github.com/benmsanderson/mices.

Miralles, D.G., Gentine, P., Seneviratne, S.I., et al., 2018. Land-atmospheric feedbacks during droughts and heatwaves: state of the science and current challenges. Ann. N. Y. Acad. Sci. https://doi.org/10.1111/nyas.13912.

Moore, J.K., Lindsay, K., Doney, S.C., et al., 2013. Marine ecosystem dynamics and biogeochemical cycling in the community earth system model [CESM1(BGC)]: comparison of the 1990s with the 2090s under the RCP4.5 and RCP8.5 scenarios. J. Clim. 26 (23), 9291−9312. https://doi.org/10.1175/jcli-d-12-00566.1.

Qin, D., 2015. China National Assessment Report on Risk Management and Adaptation of Climate Extremes and Disasters. Science Press, Beijing.

Robine, J.M., Cheung, S.L.K., Le Roy, S., et al., 2008. Death toll exceeded 70,000 in Europe during the summer of 2003. Comptes Rendus Biol. 331 (2), 171−178. https://doi.org/10.1016/j.crvi.2007.12.001.

Sanderson, B.M., Xu, Y., Tebaldi, C., et al., 2017. Community climate simulations to assess avoided impacts in 1.5 and 2°C futures. Earth. Syst. Dyn. 8 (3), 827−847. https://doi.org/10.3929/ethz-b-000191578.

Schleussner, C., Lissner, T., Fischer, E., et al., 2016. Differential climate impacts for policy-relevant limits to global warming: the case of 1.5°C and 2°C. Earth. Syst. Dyn. 7 (2), 327−351. https://doi.org/10.5194/esd-7-327-2016.

Seneviratne, S.I., Donat, M.G., Pitman, A.J., et al., 2016. Allowable CO_2 emissions based on regional and impact-related climate targets. Nature 529 (7587), 477−483. https://doi.org/10.1038/nature16542.

Shi, C., Jiang, Z., Chen, W., et al., 2018. Changes in temperature extremes over China under 1.5°C and 2°C global warming targets. Adv. Clim. Change Res. 9 (2), 120−129. https://doi.org/10.1016/j.accre.2017.11.003.

Smith, T.T., Zaitchik, B.F., Gohlke, J.M., 2013. Heat waves in the United States: definitions, patterns and trends. Climatic Change 118 (3−4), 811−825. https://doi.org/10.1007/s10584-012-0659-2.

Sun, J., 2014. Record-breaking SST over mid-North Atlantic and extreme high temperature over the Jianghuai-Jiangnan region of China in 2013. Chin. Sci. Bull. 59 (27), 3465−3470 (in Chinese).

Tao, J., Zhang, Y., Yuan, X., et al., 2013. Analysis of forest fires in Northeast China from 2003 to 2011. Int. J. Rem. Sens. 34 (22), 8235−8251. https://doi.org/10.1080/01431161.2013.837229.

Taylor, K.E., 2001. Summarizing multiple aspects of model performance in a single diagram. J. Geophys. Res. 106 (D7), 7183−7192. https://doi.org/10.1029/2000JD900719.

UNFCCC (United Nations Framework Convention Climate Change), 2015. Adoption of the Paris Agreement. https://unfccc.int/sites/default/files/resource/docs/2015/cop21/eng/l09r01.pdf.

Wang, F., Zhang, J., 2019. Heat stress response to national-committed emission reductions under the Paris Agreement. Int. J. Environ. Health Res. 16 (12), 2202. https://doi.org/10.3390/ijerph16122202.

Wang, H.L., Gan, Y.T., Wang, R.Y., et al., 2008. Phenological trends in winter wheat and spring cotton in response to climate changes in Northwest China. Agric. For. Meteorol. 148 (8−9), 1242−1251. https://doi.org/10.1016/j.agrformet.2008.03.003.

Wang, Z., Lin, L., Zhang, X., et al., 2017. Scenario dependence of future changes in climate extremes under 1.5 °C and 2 °C global warming. Sci. Rep. 7 (1) https://doi.org/10.1038/srep46432.

Wilbanks, T., Fernandez, S., Backus, G., et al., 2012. Climate change and infra- structure, urban systems, and vulnerabilities: technical report for the U.S. Department of Energy in support of the national climate assessment. https://www.esd.ornl.gov/eess/Infrastructure.pdf.

WMO (World Meteorological Organization), 2020. WMO statement on the state of the global glimate in 2019.

Wu, J., Gao, X., 2013. A gridded daily observation dataset over China region and comparison with the other datasets. Chin. J. Geophys. 56, 1102−1111. https://doi.org/10.6038/cjg20130406 (in Chinese).

Xu, Y., Gao, X., Shen, Y., et al., 2009. A daily temperature dataset over China and its application in validating a RCM simulation. Adv. Atmos. Sci. 26 (4), 763−772. https://doi.org/10.1007/s00376-009-9029-z.

Xu, Y., Zhou, B., Wu, J., et al., 2017. Asian climate change under 1.5-4°C warming targets. Adv. Clim. Change Res. 8, 99−107. https://doi.org/10.1016/j.accre.2017.05.004.

Yang, Y., Tang, J., Wang, S., et al., 2018. Differential impacts of 1.5°C and 2°C warming on extreme events over China using statistically downscaled and bias-corrected CESM low-warming experiment. Geophys. Res. Lett. 45 (18), 9852−9860. https://doi.org/10.1029/2018gl079272.

Ye, D., Yin, J., Chen, Z., et al., 2014. Spatial and temporal variations of heat waves in China from 1961 to 2010. Adv. Clim. Change Res. 5 (2), 66−73. https://doi.org/10.3724/SP.J.1248.2014.066.

Please cite this article as: ZHANG, G.-W., et al., Regional changes in extreme heat events in China under stabilized 1.5 °C and 2.0 °C global warming, Advances in Climate Change Research, https://doi.org/10.1016/j.accre.2020.08.003

Yu, R., Zhai, P., Lu, Y., 2017. Implications of differential effects between 1.5 and 2 °C global warming on temperature and precipitation extremes in China's urban agglomerations. Int. J. Climatol. 38, 2374−2385. https://doi.org/10.1002/joc.5340.

Yu, S., Xia, J., Yan, Z., et al., 2019. Loss of work productivity in a warming world: differences between developed and developing countries. J. Clean. Prod. 208, 1219−1225. https://doi.org/10.1016/j.jclepro.2018.10.067.

Zhang, G., Zeng, G., Li, C., et al., 2020. Impact of PDO and AMO on interdecadal variability in extreme high temperatures in North China over the most recent 40-year period. Clim. Dynam. 54, 3003−3020. https://doi.org/10.1007/s00382-020-05155-z.

Zhao, S., Zhou, T., Chen, X., 2020. Consistency of extreme temperature changes in China under a historical half-degree warming increment across different reanalysis and observational datasets. Clim. Dynam. 54 (3), 2465−2479. https://doi.org/10.1007/s00382-020-05128-2.

Zhu, M., Zhang, Z., Zhu, B., et al., 2020. Population and economic projections in the Yangtze River Basin based on shared socioeconomic pathways. Sustainability 12, 4202. https://doi.org/10.3390/su12104202.